Flexible Wearable Haptic Device for Enhancing Human–Robot Interaction

Xiaotian Sun, Zhantian Liang, Sitong Lu, and Jian Jiao

***Abstract*—In social human–robot interaction (HRI), touch is increasingly recognized as a critical channel for trust formation and affective haptic communication; however, most wearable haptic systems focus on task-oriented, stimulus–response functions, providing limited support for studying how identical haptic inputs are mapped to different social meanings under varying interaction contexts. To address this gap, this paper presents a wearable haptic device based on a cross-shaped, double-end-fixed symmetric PVDF bending actuator reinforced by a central PI layer. The structure efficiently converts in-plane strain into out-of-plane bending, enabling linear and stable vibration output suitable for fingertip-scale wearable integration. A digitally controlled high-voltage driver with relay isolation and PDMS-based electrical insulation ensures safe operation in direct-contact scenarios. Electromechanical characterization (50–800 V, 5–50 Hz) confirms linear voltage–displacement and voltage–force relationships, enabling precise amplitude modulation. An embodied interaction environment was developed using Pico 2 and Unity3D, in which identical physical pulses delivered to different fingers and gesture contexts were assigned context-dependent social semantic labels validated through participant rating tasks. In a within-subject study with 12 participants under counterbalanced condition order, the haptic-pattern recognition task achieved 96.78% overall accuracy, and trust scores on the TPS-HRI scale increased significantly when participants wore the glove compared with the bare condition. These findings demonstrate that flexible PVDF actuation can balance wearability, controllability, and affective expressiveness in compact haptic interfaces. The proposed system provides a reusable engineering framework for embodied affective HRI and establishes an empirical basis for understanding how identical haptic stimuli differentiate into social semantics under varying interaction contexts.**

***Index Terms*—PVDF bending actuator, wearable haptics, affective haptics, social semantics, human–robot interaction**

I. INTRODUCTION

WITH the rapid development of virtual reality (VR) and human–robot interaction (HRI), haptic feedback has increasingly been recognized as a critical channel for enhancing immersion, embodiment, and trust formation [1], [2]. Prior studies show that even in visually and acoustically realistic environments, the absence of touch limits user engagement, emotional investment, and interaction performance [3]–[5]. Concurrently, advances in affective computing and social robotics have expanded touch from a functional cue to a medium carrying social semantics [6], [7]. Neuroscience research indicates that gentle, rhythmic haptic stimulation can activate affective brain regions such as the insula and prefrontal cortex, thereby enhancing psychological closeness and trust [8]–[10]. However, most existing systems remain task-oriented or single-mode, and the semantic diversity of social touch is rarely examined systematically in controlled HRI experiments [11], [12].

In wearable haptic interfaces, one major challenge is designing actuators that are efficient, comfortable, low power, and capable of multi-point distributed feedback. Existing actuation technologies include ERM/LRA motors, electrostatic and electrotactile stimulation, pneumatic actuators, SMA/magnetostrictive materials, and piezoelectric mechanisms. Reviews indicate that pneumatic systems can provide large displacement but rely on pumps or valves that hinder everyday wearability; SMA and magnetostrictive actuators offer high force but suffer from slow response and thermal issues; electrostatic and electrotactile approaches are thin but limited by comfort and safety constraints [13]–[16].

Flexible piezoelectric materials such as polyvinylidene fluoride (PVDF) offer a more balanced trade-off among thickness, mass, bandwidth, and power consumption, making them especially suitable for fingertip-level distributed haptic feedback [17]–[19]. Under alternating electric fields, PVDF exhibits the inverse piezoelectric effect and produces perceivable micro-scale vibrations. Compared with rigid piezoceramics (e.g., PZT), PVDF provides superior flexibility, mechanical compliance, and compatibility with skin or textile substrates, offering advantages in safety and comfort for wearable applications [20]–[22].

However, most PVDF actuators adopt cantilevered or stacked configurations, requiring elevated voltages to produce practical displacement amplitudes and risking dielectric breakdown during prolonged use [23]–[25]. To overcome this structural limitation, this work proposes a wearable haptic system centered on a cross-shaped, double-end-fixed symmetric PVDF bending actuator reinforced by a central PI layer and TPU end constraints. This configuration enables efficient strain transfer, uniform stress distribution, and amplified normal-direction displacement under relatively low driving voltages. Electromechanical characterization demonstrates linear displacement–voltage behavior, low hysteresis, and stable frequency response characteristics.

On the interaction side, we develop an embodied interaction environment using Unity3D and Pico 2, in which identical physical pulses are semantically differentiated across finger locations and gesture contexts. Through haptic-pattern recognition and trust assessment using the TPS-HRI scale, we

This work was supported by the National Natural Science Foundation of China (Grant No. 52205001), the Major Key Projects of PCL under Grants (PCL2025A12-2, PCL2024A04-1), and the Guangdong S&T Program under Grant (2024B0101010003). Corresponding authors: Jian Jiao and Sitong Lu.

Xiaotian Sun, Zhantian Liang, and Sitong Lu are with the School of Mechanical and Materials Engineering, North China University of Technology, Beijing 100144, China (e-mail: 002392@ncut.edu.cn; leoliangsw@gmail.com; lusitong@ncut.edu.cn).

Jian Jiao is with Peng Cheng Laboratory, Shenzhen 518055, China (e-mail: jiaoj01@pcl.ac.cn).

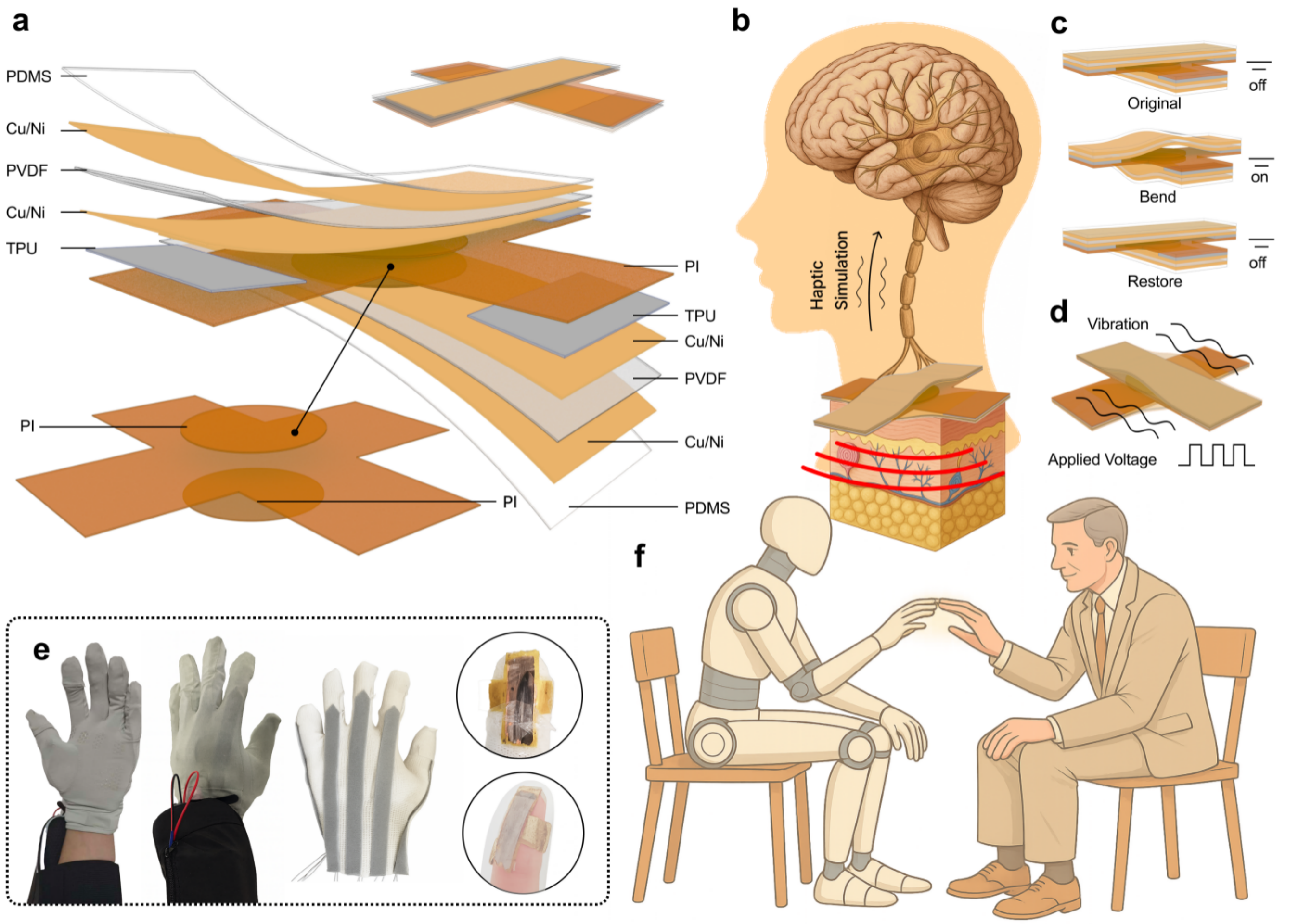

Fig. 1. Overview of the multilayer structure, actuation mechanism, glove integration, and application scenario of the proposed wearable affective haptic system. (a) Exploded view of the cross-shaped PVDF actuator. (b) Mechanoreceptor activation and affective processing in the somatosensory system. (c) Electric-field-induced bending of the PVDF actuator. (d) Out-of-plane vibration under square-wave driving. (e) PVDF modules integrated into a textile glove for multi-point feedback. (f) Wearable haptic system for social human–robot interaction.

demonstrate that tactile patterns can acquire context-dependent social semantic meanings and contribute to enhanced human–robot trust [25]–[27].

Overall, this research establishes a multi-layer wearable haptic system integrating flexible PVDF actuation and embodied affective interaction. The system bridges engineering implementation with empirical investigation of semantic differentiation in touch, providing a unified framework for future wearable social robotics and affective HRI.

II. Design of the Wearable Affective Haptic System

As shown in Fig. 1, this work first designed a cross-shaped, double-end-fixed symmetric bending actuator supported by a PI substrate with a centrally reinforced region. The structure consists of two PVDF actuation arms and a central stiffened zone, enabling efficient dual-arm vibration output within a compact form factor. The actuator uses a 50-μm-thick PI film as the substrate, with an overall size of 30×30 mm and an arm width of 10 mm.

Two 10-mm-diameter PI circular reinforcement patches are attached on both sides of the central junction to increase stiffness and maintain structural symmetry. The PVDF films (50 μm thick, 10×30 mm in size) are bonded to the PI arms using 5×10 mm TPU adhesive strips at both ends, forming a double-end-fixed bending support. Both sides of the PVDF are coated with Cu/Ni composite electrodes, where the Ni layer serves as anti-oxidation protection and the Cu layer directly interfaces with PVDF to ensure stable conductivity. The entire actuator unit is encapsulated by a 0.5-mm PDMS layer to provide electrical insulation, waterproofing, and mechanical protection.

Through the combined design of central stiffening and end-anchoring constraints, the structure effectively converts in-plane strain into out-of-plane bending displacement, significantly enhancing the normal-direction actuation sensitivity of the PVDF film. Compared with traditional cantilever configurations, the symmetric cross-shaped layout not only achieves uniform stress distribution and stable actuation behavior but also produces larger vibration amplitudes under low voltage. The central PI reinforcement helps maintain geometric symmetry and mechanical balance during actuation, preventing lateral drift and warping, and thereby improving mechanical durability and wearing comfort in wearable environments.

As shown in Fig. 1, when an electric field is applied to the PVDF layer, its molecular dipoles reorient along the polarization direction, producing the inverse piezoelectric effect and inducing reversible thickness-direction strain and bending. Under voltage, the PVDF arms bend symmetrically due to the combined effects of TPU end constraints and central PI stiffening; when the voltage is removed, internal stresses relax and the structure returns to its initial state. Under periodic square-wave driving, this process produces stable reciprocating vibration, enabling low-power and high-responsiveness tactile output.

As shown in Fig. 1, the fabricated actuator is integrated into the fingertip regions of a flexible textile glove to achieve distributed, multi-point haptic feedback. Each PVDF module corresponds to an individual finger and supports independent replacement and control. The driving electronics are placed in an arm-mounted pouch to improve comfort and portability. Through multi-channel coordinated control, different fingertip modules can generate diverse vibration patterns representing social touch behaviors such as pressing, stroking, or contacting. This modular design enables scalability from a single actuator to a full hand-based interface, providing higher emotional resolution and expressive capability for human–machine interaction.

As shown in Fig. 1, when alternating square-wave voltage is applied, the PVDF layer generates mechanical vibration corresponding to the driving frequency. The voltage amplitude determines vibration intensity, while the frequency determines perceptual rhythm. Using an Arduino microcontroller and a high-voltage boost module, the system achieves precisely adjustable tactile output in the 5–50 Hz range. This design maintains a compact structure while achieving a balance among energy efficiency, stability, and response speed, providing reliable tactile actuation for virtual interaction scenarios.

As shown in Fig. 1, haptic signals are transmitted through cutaneous mechanoreceptors (e.g., Merkel discs and Pacinian corpuscles) to the somatosensory cortex, further engaging brain regions involved in social and affective processing such as the prefrontal cortex and the insula [28]. Studies have shown that gentle, rhythmic haptic stimulation can induce positive affective arousal, promote trust formation, and facilitate social empathy responses [29], [30]. Thus, the system provides not only physical tactile feedback but also a pathway through which tactile signals may contribute to affective interpretation in social HRI contexts.

The system serves as an affective communication interface in social HRI scenarios. When a human wearing the haptic glove interacts with a robot, different vibration patterns correspond to context-dependent social meanings such as soothing, connecting, or granting permission. Through this embodied haptic language, the robot participates in social interaction by conveying context-dependent social cues and enhancing its perceived social presence.

In summary, this section presents a multilayer design logic spanning materials, structure, actuation mechanism, wearable integration, and affective perception. Through the centrally reinforced cross-shaped double-end-fixed PVDF actuator, its multilayer construction, electromechanical conversion mechanism, multi-channel glove integration, and programmable control, the proposed system achieves expressive and perceivable affective haptic feedback. It not only provides precise and controllable tactile stimulation at the physical level but also supports social-semantic affective expression, offering a new theoretical and application pathway for affective robotics and embodied computing.

III. Fabrication and Wearable Integration of the PVDF-Based Haptic Actuator

Fig. 2 illustrates the fabrication process of the PVDF-based haptic actuator. A 50-μm-thick PVDF film with dimensions of 10×30 mm was selected, and both sides were coated with Cu/Ni composite electrodes, where the Ni layer served as the outer protective coating and the Cu layer directly contacted the PVDF to form a stable conductive interface. To prevent short-circuiting under high-voltage driving and to reduce edge effects, the two sides of the film were masked with approximately 8×28 mm adhesive tape before immersing the sample in a ferric chloride ($FeCl_3$) solution for electrode-edge etching. After etching, the tape was removed, resulting in a PVDF film with an effective working region of approximately 8×28 mm, featuring well-defined electrode boundaries and reliable insulation performance.

Subsequently, a cross-shaped substrate with an overall size of 30×30 mm and an arm width of 10 mm was laser-cut from a 50-μm-thick polyimide (PI) film. Two PI circular reinforcement patches (10-mm diameter) were adhered to both sides of the central junction to enhance the stiffness of the connection area and maintain structural symmetry. Two strips of thermoplastic polyurethane (TPU) adhesive tape (5×10 mm) were placed on opposite arms of the PI substrate to anchor the two ends of the PVDF film. After precisely aligning the PVDF film along its polarization direction, the film was gently pressed onto the TPU at room temperature to ensure firm bonding while avoiding thermal deformation. Fine copper wires were soldered onto the PVDF electrodes to establish electrical connections.

A layer of polydimethylsiloxane (PDMS) with a thickness of approximately 0.5 mm was then uniformly applied to both sides of the device to provide insulation, waterproofing, and mechanical protection. After fabrication, the completed PVDF actuator was embedded into the fingertip region of a fabric glove (as shown in Fig. 2) and secured inside the glove using Velcro, ensuring stable contact with the skin while maintaining wearing comfort. Flexible wires were routed along the outer surface of the glove and connected to a wrist-mounted control module. This fabrication and integration process is simple and reproducible, providing effective electrical insulation and controllable actuation behavior, and is well suited for wearable tactile interfaces in human–machine interaction scenarios.

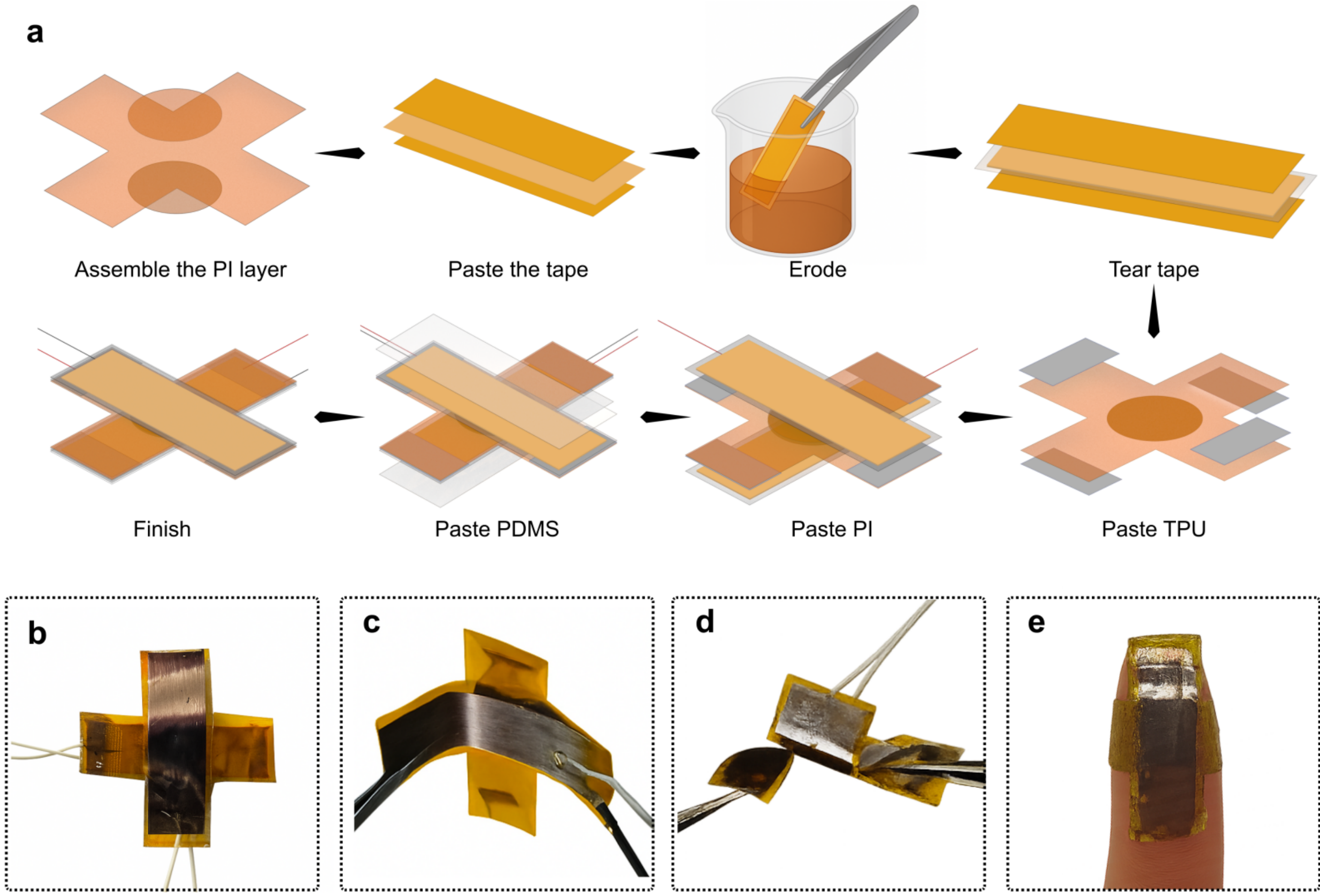

Fig. 2. Fabrication and wearable integration process of the PVDF-based haptic actuator. (a) Fabrication workflow of the PVDF actuator. (b) Front view of the fully assembled cross-shaped actuator. (c)–(d) Mechanical response of the actuator under different bending states. (e) Demonstration of the PVDF actuator attached to the fingertip.

IV. Electromechanical Performance Testing and Analysis of the PVDF Actuator

Fig. 3 presents the electromechanical response characteristics of the PVDF-based tactile actuator under various driving conditions. The primary output parameters—tip displacement and force—were measured using a Panasonic HL-G103-S-J laser displacement sensor and a DSZ-100 (0.5 kg) force sensor, respectively. Experiments were performed across voltage amplitudes from 50 V to 800 V and driving frequencies from 5 Hz to 50 Hz.

As shown in Fig. 3, both displacement and output force increase approximately linearly with voltage, indicating efficient electromechanical energy conversion without signs of dielectric saturation within the tested voltage range. Under a constant voltage, the displacement amplitude gradually decreases as frequency increases, whereas the maximum output force occurs at 5 Hz and 800 V, corresponding to the highest mechanical energy transfer efficiency. At higher frequencies, a slight reduction in output force is observed due to the mechanical inertia and internal damping of the PVDF film, which limit full bending–recovery motion within each cycle. Additionally, polarization reorientation lag at high frequencies further reduces electromechanical conversion efficiency, resulting in progressive attenuation of force output.

To further examine the actuator's time-domain characteristics, a representative operating condition of 200 V and 10 Hz was selected. This operating point lies within the actuator's low-voltage stable region, avoiding dielectric nonlinearity and high-voltage noise while providing sufficient displacement and force amplitude to clearly demonstrate the periodic actuation waveform. As shown in Fig. 3, both displacement and force exhibit regular, sinusoidal waveforms with clear periodicity and strong repeatability, indicating good synchronization between electrical excitation and mechanical deformation. Even under low-voltage, high-frequency conditions (50 Hz, 200 V), the actuator still produces detectable and stable force output, demonstrating its high sensitivity and efficient energy conversion under low driving voltages.

Overall, the results in Fig. 3 show that the displacement and output force of the double-end-fixed PVDF actuator increase linearly within the 0–800 V range. Across the 5–50 Hz frequency band, displacement amplitude decreases with increasing frequency, while force output exhibits only mild attenuation. Time-domain waveforms display excellent cycle-to-cycle consistency and minimal phase lag, confirming synchronized electrical–mechanical response. Unlike cantilever-

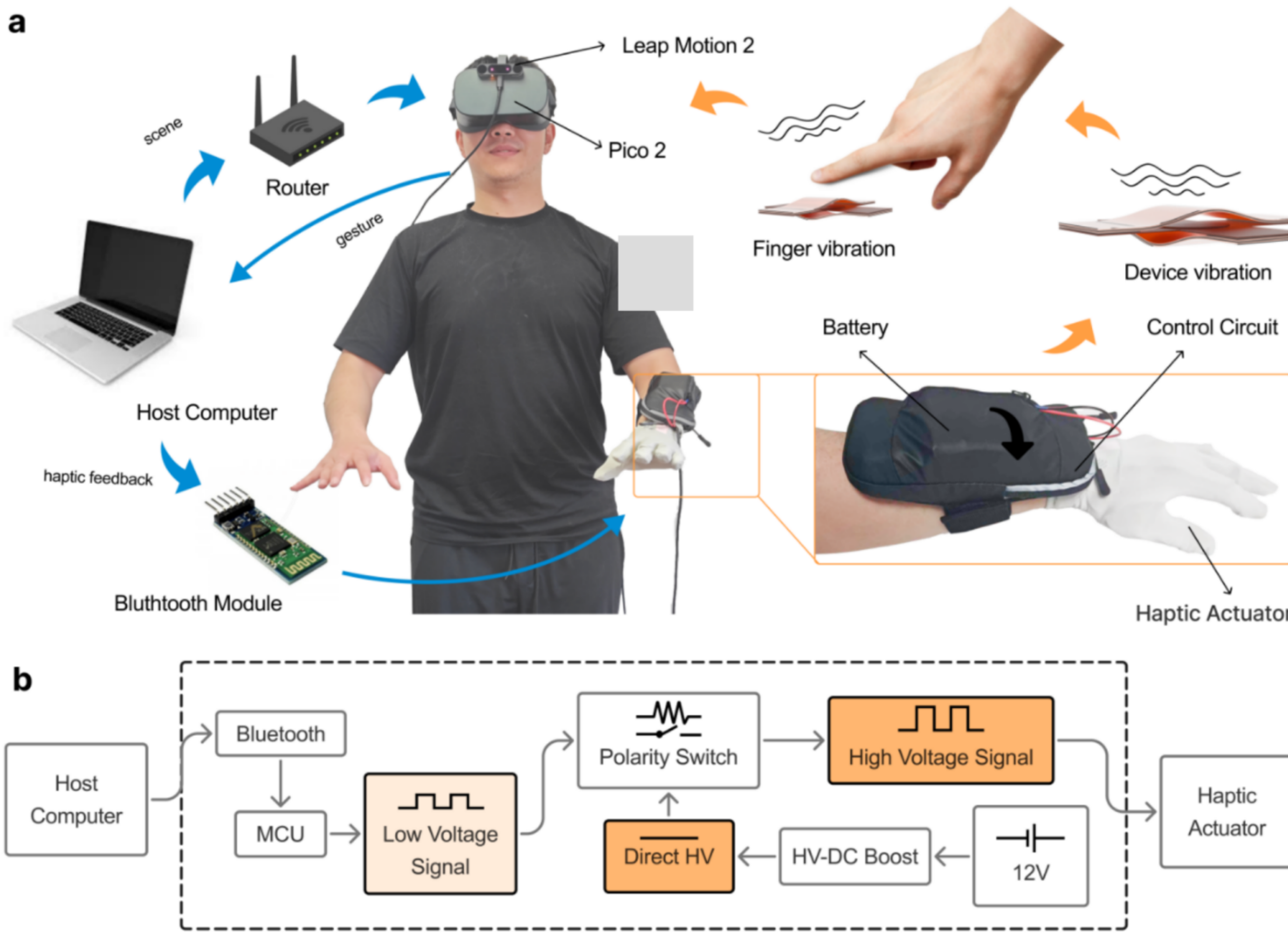

Fig. 3. Electromechanical performance of the PVDF-based tactile actuator. (a) Experimental setup for measuring tip displacement and output force. (b)–(i) Voltage- and frequency-dependent electromechanical responses of the actuator.

type structures that often exhibit strong resonance peaks in specific bands, the double-end-fixed and centrally reinforced configuration shows no pronounced resonance behavior. The increased structural stiffness and inherent damping suppress resonance modes, leading to a quasi-static piezoelectric response dominated by electric-field-induced bulk strain rather than mechanical resonance amplification [14], [15].

In summary, the PVDF-based tactile actuator achieves stable, linear, and controllable vibration output under low to moderate driving voltages, with high sensitivity, low power consumption, and strong mechanical reliability. These characteristics establish a solid hardware foundation for subsequent tactile-feedback and human–machine interaction studies [15].

V. Haptic Actuator System Architecture and Control Circuit Design of the PVDF-Based Haptic Glove

To realize the embodied-interaction framework outlined in the Introduction, the haptic glove system was designed to tightly couple user gesture states, virtual scene events, and fingertip tactile feedback within a closed-loop VR environment. The architecture maintains constant physical stimulation parameters while systematically varying interaction context—such as contact location and gesture type—thereby enabling controlled examination of context-dependent haptic perception and social meaning attribution. Accordingly, the system integrates real-time hand tracking, wireless control, and digitally driven PVDF actuation into a compact wearable platform. Fig. 4 illustrates the system architecture and control circuit design of the PVDF-based tactile glove. The system primarily consists of a host computer, a VR headset (Pico 2), a hand-tracking module (Leap Motion 2), and PVDF tactile actuation units. The host computer handles virtual-scene rendering and interaction-logic control, synchronizes with the Pico 2 via a wireless router, and receives hand-motion data captured by the Leap Motion 2. When the user performs an action in the virtual environment, the host computer generates corresponding haptic-feedback commands based on the real-time gesture state and wirelessly transmits them to the wearable microcontroller unit (MCU). The MCU modulates the driving signal according to the received commands and controls the PVDF actuators to output mechanical vibrations of specific frequencies and amplitudes, thereby forming an interaction pipeline of gesture action $\rightarrow$ virtual feedback $\rightarrow$ tactile perception. With the glove

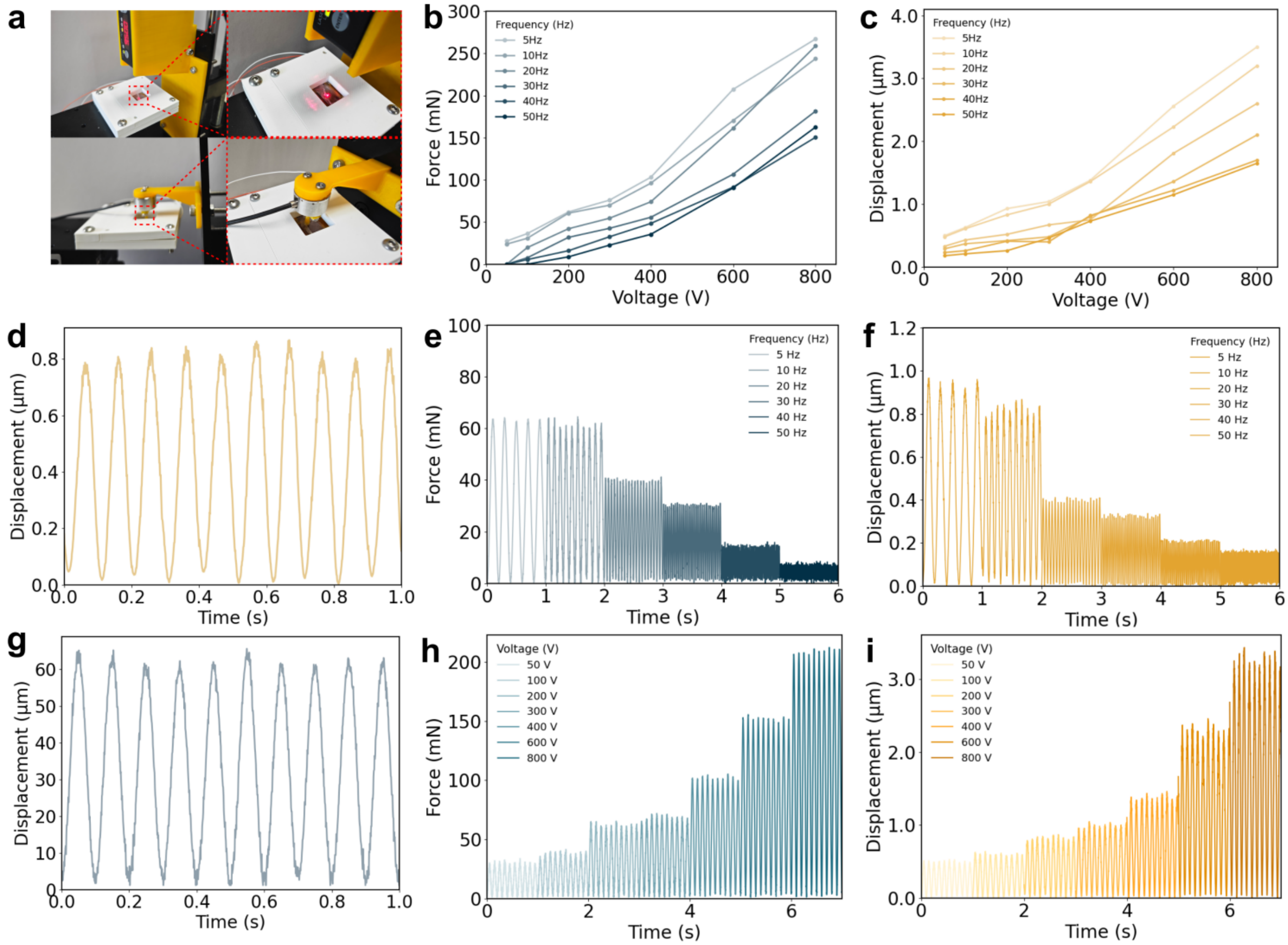

Fig. 4. System architecture and control circuit design of the PVDF-based haptic glove. (a) System architecture. (b) Control circuit block diagram.

worn, users can experience synchronized motion control and physical tactile feedback in VR, achieving a more natural and immersive interaction experience.

The control circuit, shown in Fig. 4, is designed to generate stable high-voltage pulse driving under digital control. The system uses an Arduino UNO microcontroller as the core, combined with a Bluetooth communication module (HC-05), a mechanical relay, a high-voltage DC boost converter (HV-DC Boost), and a power-supply unit to form a compact driving module. The host computer wirelessly transmits tactile-feedback commands to the MCU via Bluetooth. The MCU outputs a pulse-width-modulated (PWM) signal corresponding to the target vibration frequency, directly controlling the relay switching state. The relay periodically connects or disconnects the output of the HV-DC boost module, allowing high-voltage pulses to be applied to the PVDF film at the set frequency. When the relay is ON, the boost converter steps up the 12-V DC input to 0–2000 V and applies it across the PVDF film, causing bending deformation under the electric field. When the relay is OFF, the high voltage is cut off and the film returns to its initial state. Periodic switching enables stable, controllable mechanical vibration in the 5–50 Hz range. This unipolar high-voltage pulse-driving approach achieves effective actuation without polarity reversal, featuring a simple structure and stable response. The PWM frequency determines the vibration rhythm, and the duty cycle can be used to modulate driving intensity.

To ensure operational safety, multiple protection measures are implemented. The high-voltage output current is limited to below 1 mA, and the output power of the high-voltage module is kept under 2 W. The electrode layout is optimized such that the negative terminal (ground) faces the skin-contact side, reducing electric-shock risk. A ∼0.5-mm-thick PDMS insulation layer is coated on the device surface to enhance electrical insulation and mechanical protection. The entire driving circuit is fixed and integrated into an arm-mounted pouch to improve wearability and user comfort. The overall system is compact, safe, and reliable, capable of delivering stable high-voltage pulse signals and providing precise and repeatable tactile actuation for wearable human–machine interaction experiments.

VI. Immersive Virtual Narrative System for Social Human–Robot Interaction

After completing hardware integration and performance calibration, an immersive virtual narrative system was developed in Unity3D to examine how identical haptic pulses

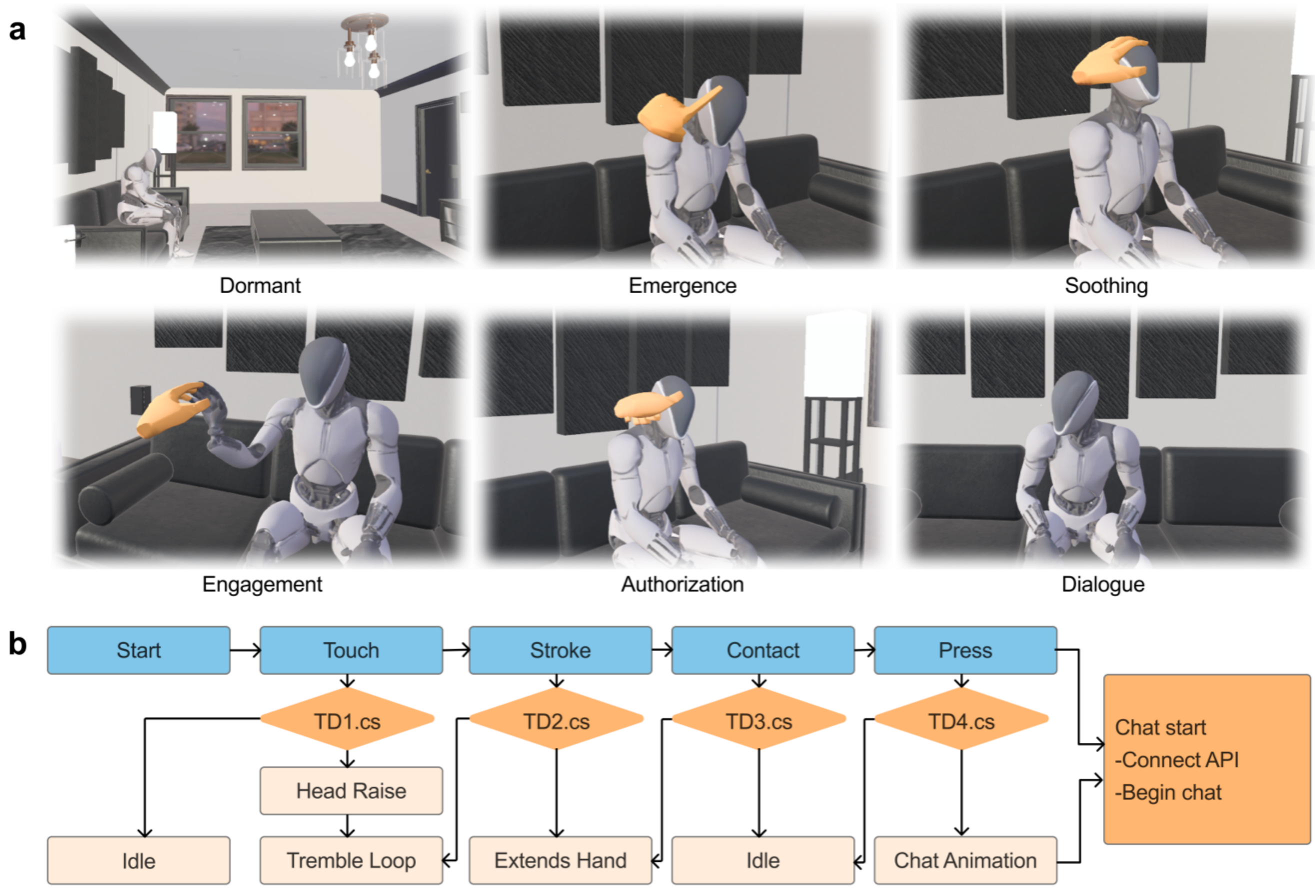

Fig. 5. Immersive virtual narrative system and social tactile interaction design. (a) Immersive VR meeting environment constructed in Unity3D. (b) Gesture-triggered interaction logic.

are perceived and assigned different social meanings under varying interaction contexts. The system runs on a Pico 2 headset, uses Leap Motion to track skeletal hand movements, and delivers real-time vibration feedback through a PVDF-based haptic glove, thereby achieving synchronized coupling between visual motion and tactile feedback.

As shown in Fig. 5, the virtual environment simulates a quiet indoor setting in which the robot remains in a Dormant state, exhibiting no social behaviors. When the user's index-finger tip maintains contact with the robot's forehead for at least 1.0 s, a collision event is detected and TD1.cs is executed, triggering a 200 V, 10 Hz vibration on the index finger alone. The robot transitions into the Emergence state, showing slight trembling—resembling the tension of a newborn—along with signs of attentional awakening, marking the initiation of the interaction. If the user performs three or more finger–surface contacts within a 0.5-s window, the system classifies the gesture as stroking and executes TD2.cs, driving all five fingers with the same 200 V, 10 Hz pattern. The robot enters the Soothing state, gradually relaxing from initial tension and displaying behaviors associated with affective regulation. When the four fingertips (excluding the thumb) simultaneously contact the robot's palm, TD3.cs is triggered, producing synchronized vibration on the four corresponding fingers. The robot shifts into the Engagement state, extending its arm toward the user as a sign of relational commitment and willingness to interact. Finally, when the user's thumb tip presses against the robot's forehead, TD4.cs is activated, again producing a fixed 200 V, 10 Hz vibration on the thumb while simultaneously calling an external API. This event transitions the robot into the Authorization state and subsequently into the Dialogue state, enabling the robot to move from passive reactivity to active communication.

Throughout the entire narrative, all haptic feedback is delivered using identical stimulation parameters (200 V, 10 Hz), ensuring constant physical intensity. Consequently, differences in perceived social meaning arise solely from the interaction context of the gestures, rather than from differences in vibration amplitude. The four user-initiated touch gestures correspond to common categories of social touch—exploratory touch, stroking, palm-to-palm contact, and confirmatory pressing—forming a continuous socio-emotional trajectory from "emergence of intelligence," to "affective soothing," "relational engagement," and finally "authorization and dialogue." Through this embodied and sequential narrative structure, the system achieves a semantic remapping of tactile signals: the same

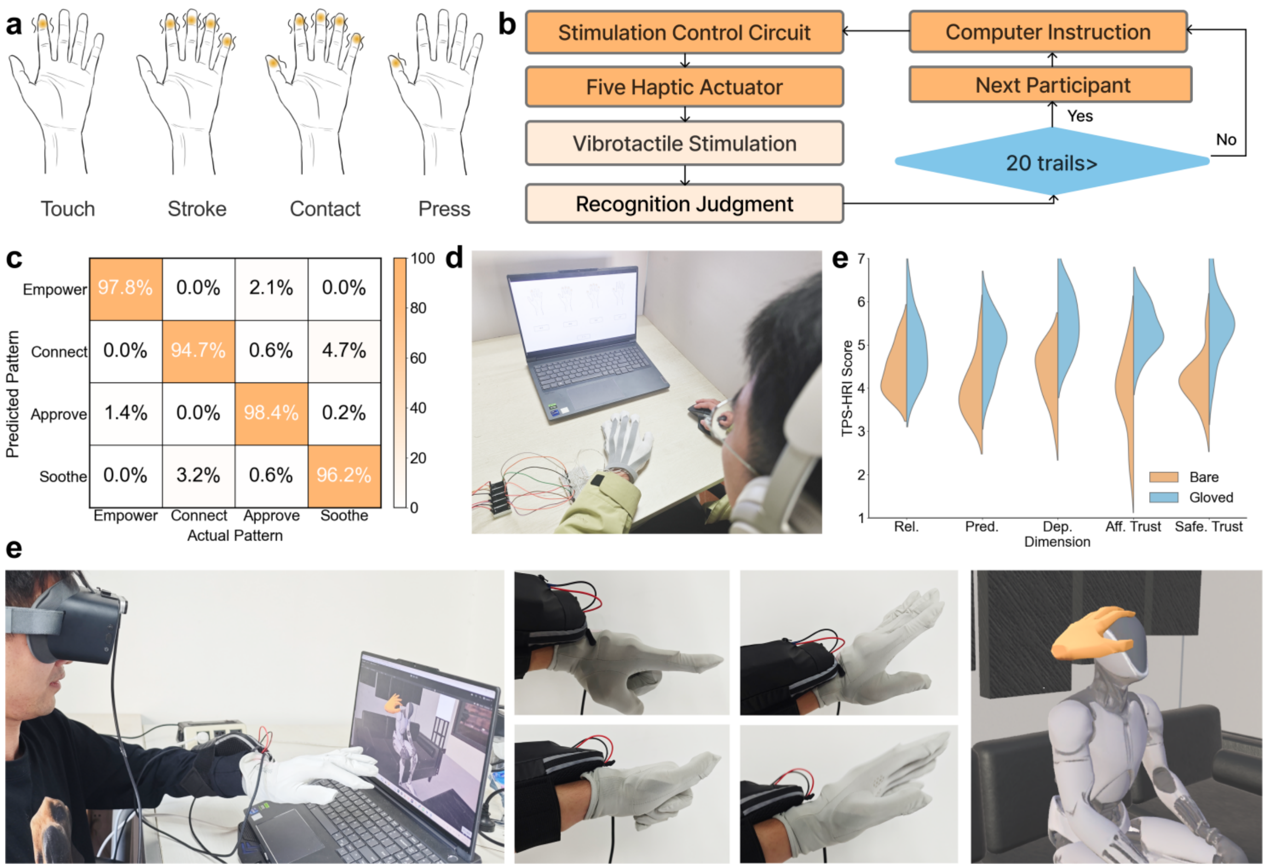

Fig. 6. Experimental design and results for tactile pattern recognition and trust evaluation. (a) The four vibrohaptic stimulation patterns used in the recognition task. (b) Flowchart of the recognition experiment. (c) Confusion matrix showing high overall recognition accuracy (96.8%) across the four haptic patterns. (d) Experimental setup for the recognition task. (e) Trust evaluation results in the narrative interaction task (adapted from TPS-HRI).

PVDF vibration pulse acquires different social meanings under different interaction contexts. This provides a controlled and reproducible experimental framework for investigating how social touch mediates trust formation, emotional bonding, and active engagement in HRI.

VII. Evaluation of Haptic Discriminability and Narrative-Based Trust in HRI

Fig. 6 presents the experimental design and results of the human–robot interaction study conducted with the PVDF-based haptic glove. Two experiments were performed: a forced-choice haptic-pattern recognition experiment to evaluate the discriminability of the multi-actuator glove, and a narrative-driven dynamic trust experiment to examine how haptic feedback shapes trust formation across consecutive social interaction stages. Twelve healthy adult participants (6 male, 6 female, aged 21–26) were recruited, all with normal haptic perception and no neuromuscular or upper-limb impairments.

In the haptic recognition experiment, four actuator activation patterns were randomly presented to the participants (Fig. 6): Touch (single-finger vibration), Stroke (five-finger vibration), Contact (four-finger vibration excluding the thumb), and Press (thumb vibration). These patterns were presented only as physical labels without any narrative or symbolic meaning to avoid semantic bias. All haptic stimuli were delivered with fixed parameters (10 Hz, 200 V, 2 s). Participants wore active noise-cancelling headphones and used their left hand to avoid dominance-related sensitivity differences. Each participant completed 20 randomized trials (4 patterns $\times$ 5 repetitions). After each stimulus, participants selected the perceived pattern from a graphical interface, and both accuracy and reaction time were recorded; a 3 s interval was applied between stimuli. As shown in Fig. 6, the overall recognition accuracy reached 96.8%, significantly above the 25% chance level (χ^2 test, $p < 0.001$). The accuracy rates for the four patterns were 97.9% (Touch), 96.2% (Stroke), 94.7% (Contact), and 98.4% (Press). The primary confusion occurred between Stroke and Contact (4.7% and 3.2%), consistent with their partially overlapping spatial activation regions. Reaction time showed no systematic downward trend, suggesting no measurable learning effect. These results support the glove's ability to deliver stable and reliably distinguishable multi-channel haptic feedback.

Building on this, a narrative-based dynamic trust experiment (Fig. 6) was conducted to assess how haptic feedback influences trust formation across a continuous social interaction sequence. Participants interacted with a virtual robot in a VR environment through a six-stage narrative progression—Dormant → Emergence → Soothing → Engagement → Authorization → Dialogue—designed to model a gradual shift from passive presence to progressively increasing social agency [31]. Two experimental conditions were tested: a Bare condition, in which participants did not wear the glove and received only visual and motion cues, and a Gloved condition, in which the PVDF glove delivered stage-specific haptic patterns. The order of the two conditions was counterbalanced across participants. Haptic patterns were mapped to narrative stages based on their intuitive social-touch characteristics: Touch (index-finger vibration) for Emergence, Stroke (five-finger vibration) for Soothing, Contact (four-finger vibration) for Engagement, and Press (thumb vibration) for Authorization, while no haptic output was provided during Dialogue [32]. All haptic patterns were delivered with identical physical parameters (200 V, 10 Hz) to ensure that differences in emotional interpretation arose from contextual meaning rather than physical intensity.

After completing the full six-stage narrative sequence, participants rated their trust in the robot using five single-item subscales adapted from the Trust Perception Scale for HRI [25]: Reliability, Predictability, Dependability, Affective Trust, and Safety Trust. Each subscale was rated on a 7-point Likert item, providing a multidimensional assessment of overall trust for each condition. A paired comparison between conditions showed that trust scores across all five TPS-HRI subdimensions were significantly higher in the Gloved condition than in the Bare condition (paired t-tests, $p < 0.05$). This indicates that the addition of haptic feedback enhanced participants' perceived reliability, predictability, dependability, affective warmth, and safety of the robot. Subjective feedback further suggested that haptic feedback increased the robot's perceived responsiveness and strengthened the continuity of the interaction.

Together, these results indicate that the PVDF-based haptic glove provides high-fidelity multi-pattern haptic cues that can enhance trust development in socially structured human–robot interactions. The finding that identical haptic pulses (200 V, 10 Hz) were interpreted differently across narrative contexts suggests a strong contextual dependence of haptic meaning. The system therefore provides a controlled and reproducible platform for studying how social touch contributes to relational processes, affective calibration, and active engagement in HRI.

VIII. Conclusion

This work presented a flexible wearable haptic device based on a cross-shaped, double-end-fixed PVDF actuator integrated into a multi-point glove interface. The actuator provides stable, linear haptic output suitable for distributed fingertip feedback. Within an immersive narrative interaction framework, we showed that identical haptic pulses acquire different social meanings depending on their contextual embedding. User studies demonstrated high haptic-pattern discriminability (96.8%) and significantly higher TPS-HRI trust scores when participants wore the glove. These results highlight the role of context in shaping haptic interpretation and establish a reproducible platform for studying social-semantic touch in human–robot interaction.

References

[1] C. Pacchierotti, F. Chinello, K. Koumaditis, M. Di Luca, E. Ofek, and O. Georgiou, "Guest editorial haptics in the metaverse: Haptic feedback for virtual, augmented, mixed, and eXtended realities," *IEEE Transactions on Haptics*, 2024.

[2] Y. Shi and G. Shen, "Haptic sensing and feedback techniques toward virtual reality," *Research*, vol. 7, p. 0333, 2024.

[3] X. Yu, Z. Xie, Y. Yu *et al.*, "Skin-integrated wireless haptic interfaces for virtual and augmented reality," *Nature*, vol. 575, pp. 473–479, 2019.

[4] G. Richard, T. Pietrzak, F. Argelaguet, A. Lécuyer, and G. Casiez, "Studying the role of haptic feedback on virtual embodiment in a drawing task," *Frontiers in Virtual Reality*, vol. 1, p. 573167, 2021.

[5] C. du Pasquier, L. Tessmer, I. Scholl, L. Tilton, T. Chen, S. Tibbits, and A. Okamura, "Haptiknit: Distributed stiffness knitting for wearable haptics," *Science Robotics*, vol. 9, no. 97, p. eado3887, 2024.

[6] M. E. Cansev, A. J. Miller, J. D. Brown, and P. Beckerle, "Implementing social and affective touch to enhance user experience in human-robot interaction," *Frontiers in Robotics and AI*, vol. 11, p. 1403679, 2024.

[7] C. Pacchierotti, S. Sinclair, M. Solazzi, A. Frisoli, V. Hayward, and D. Prattichizzo, "Wearable haptic systems for the fingertip and the hand: Taxonomy, review, and perspectives," *IEEE Transactions on Haptics*, vol. 10, no. 4, pp. 580–600, 2017.

[8] I. Valori, M. M. Jung, and M. T. Fairhurst, "Social touch to build trust: A systematic review of technology-mediated and unmediated interactions," *Computers in Human Behavior*, vol. 153, p. 108121, 2024.

[9] I. Gordon, A. C. Voos, R. H. Bennett, D. Z. Bolling, K. A. Pelphrey, and M. D. Kaiser, "Brain mechanisms for processing affective touch," *Human Brain Mapping*, vol. 34, no. 4, pp. 914–922, 2013.

[10] J. H. Kryklywy, P. Vyas, K. E. MacLean, and R. M. Todd, "Characterizing affiliative touch in humans and its role in advancing haptic design," *Annals of the New York Academy of Sciences*, vol. 1528, no. 1, pp. 29–41, 2023.

[11] M. Shiomi and H. Sumioka, *Social Touch in Human–Robot Interaction: Symbiotic Touch Interaction Between Human and Robot*. Taylor & Francis, 2024.

[12] G. Huisman, "Social touch technology: A survey of haptic technology for social touch," *IEEE Transactions on Haptics*, vol. 10, no. 3, pp. 391–408, 2017.

[13] Y. Guo, Y. Luo, R. Plamthottam, S. Pei, C. Wei, Z. Han, J. Fan, M. Possinger, K. Liu, Y. Zhu, and Z. Fei, "Haptic artificial muscle skin for extended reality," *Science Advances*, vol. 10, no. 43, p. eadr1765, 2024.

[14] N. Vanichvoranun, H. Lee, S. Kim, and S. H. Yoon, "EStatiG: Wearable haptic feedback with multi-phalanx electrostatic brake for enhanced object perception in VR," *Proc. ACM Interact. Mob. Wearable Ubiquitous Technol.*, vol. 8, no. 3, pp. 1–29, 2024.

[15] Q. Liu, S. Ghodrat, G. Huisman, and K. M. Jansen, "Shape memory alloy actuators for haptic wearables: A review," *Materials & Design*, vol. 233, p. 112264, 2023.

[16] J. H. Youn, S. Y. Jang, I. Hwang, Q. Pei, S. Yun, and K. U. Kyung, "Skin-attached haptic patch for versatile and augmented tactile interaction," *Science Advances*, vol. 11, no. 12, p. eadt4839, 2025.

[17] B. Chen, Z. Feng, F. Z. Yao, M. H. Zhang, K. Wang, Y. Wei, W. Gong, and J. Rödel, "Flexible piezoelectrics: Integration of sensing, actuating and energy harvesting," *npj Flexible Electronics*, vol. 9, no. 1, p. 58, 2025.

[18] Y. Wu, Y. Ma, H. Zheng, and S. Ramakrishna, "Piezoelectric materials for flexible and wearable electronics: A review," *Materials & Design*, vol. 211, p. 110164, 2021.

[19] H. Jin, Y. Kim, W. Youm, Y. Min, S. Seo, C. Lim, C. H. Hong, S. Kwon, G. Park, S. Park, and H. J. Kim, "Highly pixelated, untethered tactile interfaces for an ultra-flexible on-skin telehaptic system," *npj Flexible Electronics*, vol. 6, no. 1, p. 82, 2022.

[20] F. Qi, L. Xu, Y. He, H. Yan, and H. Liu, "PVDF-based flexible piezoelectric tactile sensors," *Crystal Research and Technology*, vol. 58, no. 10, p. 2300119, 2023.

[21] W. Fan, R. Lei, H. Dou, Z. Wu, L. Lu, S. Wang, X. Liu, W. Chen, M. Rezakazemi, T. M. Aminabhavi, and Y. Li, "Sweat permeable and ultrahigh strength 3D PVDF piezoelectric nanoyarn fabric strain sensor," *Nature Communications*, vol. 15, no. 1, p. 3509, 2024.

[22] Y. Chen, X. Zhang, and C. Lu, "Flexible piezoelectric materials and strain sensors for wearable electronics and artificial intelligence applications," *Chemical Science*, 2024.

[23] T. Gao, Q. Liao, W. Si, Y. Chu, H. Dong, Y. Li, Y. Liao, and L. Qin, "From fundamentals to future challenges for flexible piezoelectric actuators," *Cell Reports Physical Science*, vol. 5, no. 2, 2024.

[24] H. Ding, D. Yang, S. Ding, and F. Ma, "Reprogrammable flexible piezoelectric actuator arrays with a high degree of freedom for shape morphing and locomotion," *Soft Robotics*, 2025.

[25] K. E. Schaefer, "Measuring trust in human robot interactions: Development of the 'trust perception scale-HRI'," in *Robust Intelligence and Trust in Autonomous Systems*, Boston, MA, USA: Springer, 2016, pp. 191–218.

[26] C. Cirasa and D. Conti, "Mapping trust and cultural dimensions in human-robot interaction: A scoping review approach," *Computers in Human Behavior Reports*, p. 100763, 2025.

[27] J. Plomin, P. Schweidler, and A. Oehme, "Virtual reality check: A comparison of virtual reality, screen-based, and real world settings as research methods for HRI," *Frontiers in Robotics and AI*, vol. 10, p. 1156715, 2023.

[28] M. Björnsdotter, I. Gordon, K. A. Pelphrey, H. Olausson, and M. D. Kaiser, "Development of brain mechanisms for processing affective touch," *Frontiers in Behavioral Neuroscience*, vol. 8, p. 24, 2014.

[29] L. Mayorova, G. Portnova, and I. Skorokhodov, "Cortical response variation with social and non-social affective touch processing in the glabrous and hairy skin of the leg: A pilot fMRI study," *Sensors*, vol. 23, no. 18, p. 7881, 2023.

[30] C. Krahé, M. von Mohr, A. Gentsch, L. Guy, C. Vari, T. Nolte, and A. Fotopoulou, "Sensitivity to CT-optimal, affective touch depends on adult attachment style," *Scientific Reports*, vol. 8, no. 1, p. 14544, 2018.

[31] I. Leite, C. Martinho, and A. Paiva, "Social robots for long-term interaction: A survey," *International Journal of Social Robotics*, vol. 5, no. 2, pp. 291–308, 2013.

[32] T. Field, "Touch for socioemotional and physical well-being: A review," *Developmental Review*, vol. 30, no. 4, pp. 367–383, 2010.

Xiaotian Sun received the Ph.D. degree in Design Strategy from Kyushu University, Fukuoka, Japan, in 2019, the M.A. degree in Information Experience Design from the Royal College of Art, London, U.K., and the B.Eng. degree in Industrial Design from Dalian University of Technology, Dalian, China. She is currently a Lecturer and Master's Supervisor with the School of Mechanical and Materials Engineering, North China University of Technology, Beijing, China, and also a Visiting Scholar with the Design and Augmented Intelligence Lab at Cornell University, Ithaca, NY, USA, since 2025. Her research interests include embodied interaction, informatized haptics, olfactory and gustatory interaction design, as well as industrial design and information experience.

Zhantian Liang focuses on embodied interaction and affective haptic systems for social human–robot interaction, with the aim of enabling robots to generate more subtle and expressive forms of haptic feedback. By integrating multiple actuation mechanisms and systematically exploring their tactile characteristics, he investigates interaction systems capable of conveying nuanced variations in emotion, intention, and social presence. His work contributes to the development of socially expressive robotic systems in which touch functions not only as a sensory interface but also as an important medium for emotional expression and interpersonal communication.

Sitong Lu received the Ph.D. degree from Beihang University (Beijing University of Aeronautics and Astronautics), Beijing, China, the M.S. degree from Nanyang Technological University, Singapore, and the B.S. degree from Dalian University of Technology, Dalian, China. She is currently a Lecturer and Master's Supervisor with North China University of Technology, Beijing, China. She is a member of the China Computer Federation (CCF). She has been the Principal Investigator of one National Natural Science Foundation of China (NSFC) Young Scientists Fund project and has participated in multiple national and provincial research projects. Her research focuses on flexible sensing technology, especially flexible multimodal sensing electronic devices and wearable technology.

Jian Jiao received the Ph.D. degree in Mechanical Engineering from Beihang University, Beijing, China, in 2019. He was a visiting Ph.D. student at the University of California, USA, in 2018. He is currently an Associate Professor and Doctoral Supervisor at Peng Cheng Laboratory, Shenzhen, China. He has served as a Young Editorial Board Member for *Wearable Electronics* since 2024, and for *Soft Science* since 2025. He has been a reviewer of *IEEE Transactions on Industrial Informatics* since 2023. His research interests include soft robotics, flexible electronics, haptics, virtual reality, and embodied intelligence.